Highly efficient production and purification of fructose via glucose isomerization by calcium chloride and triethylamine

Zhaohui Guo, [a,b] Christian Marcus Pedersen, [c] Honghong Chang, [d] Yingxiong Wang, [*a,e] and Yan Qiao[*a,b]

[a] *State Key Laboratory of Coal Conversion, Institute of Coal Chemistry, Chinese Academy of Sciences, 27 South Taoyuan Road, Taiyuan 030001, China*

[b] *Center of Materials Science and Optoelectronics Engineering, University of Chinese Academy of Sciences, Beijing 100049, China*

[c] *Department of Chemistry, University of Copenhagen, Universitetsparken 5, DK-2100 Copenhagen, Denmark*

[d] *Shanxi Tihondan Pharmaceutical Technology Co., Ltd., Jinzhong 030600, China*

[e] *College of Chemistry, Taiyuan University of Technology, 79 Yingze West Street, Wanbailin District, Taiyuan 030024, China*

* Corresponding Author. E-mail addresses: wangyingxiong@tyut.edu.cn (Y. Wang), qiaoy@sxicc.ac.cn (Y. Qiao).

NMR section

In DEPT135 NMR spectrum, the phase of the signals corresponding to -CH_3 and -CH is different from the signals corresponding to -CH_2. The signal of -CH_3 and -CH are upward, and the signal of -CH_2 is downward, the quaternary carbon atom not attached to hydrogen show no signal.

$^{1}H-^{13}C$ HSQC NMR spectrum shows the signals that ^{13}C and ^{1}H correlated points. In phase sensitive HSQC NMR, the peaks from -CH or -CH_3 are different from -CH_2 in phase, which define as two different colors on the spectrum.

DOSY (Diffusion ordered spectroscopy) experiments were performed with the Bruker standard bipolar pulse longitudinal eddy current delay (BPPLED) pulse sequence. The relaxation delay time was 2000 ms, and the diffusion time (Δ) was 100−300 ms according to the properties of samples. The duration of the pulse field gradient (δ/2) was adjusted to be in the range of 1000−2000 μs in order to obtain 2−5% residual signal with the maximum gradient strength. The delay for gradient recovery was 0.2 ms, and the eddy current delay was 5 ms. The gradient strength was incremented in 16 steps from 2% to 95% of its maximum value in a linear ramp.

According to the Stokes-Einstein equation: $$D = \frac{kT}{6\pi\eta r_s}$$

in which k is the Boltzmann constant, T is the temperature, η is the viscosity of the liquid, and r_s is the hydrodynamic radius of the molecule. The obtained diffusion coefficient (D) value of a species in solution from DOSY experiment is dependent on the molecular weight and size.

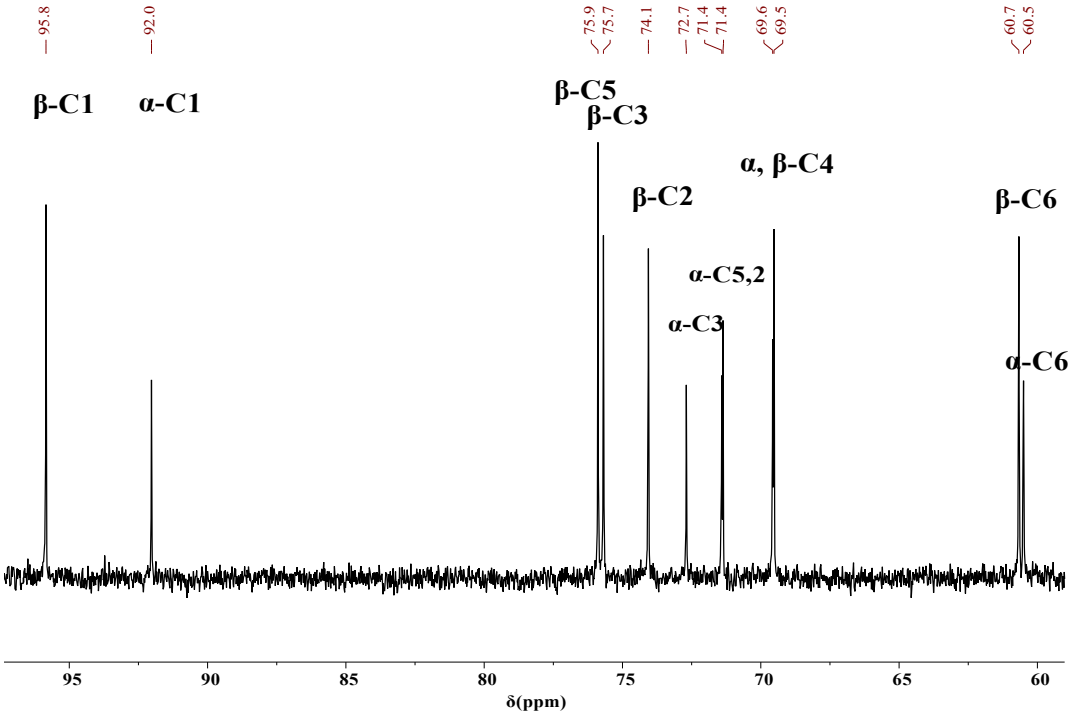

Figure S1. ^{13}C NMR spectrum for glucose in D_2O.

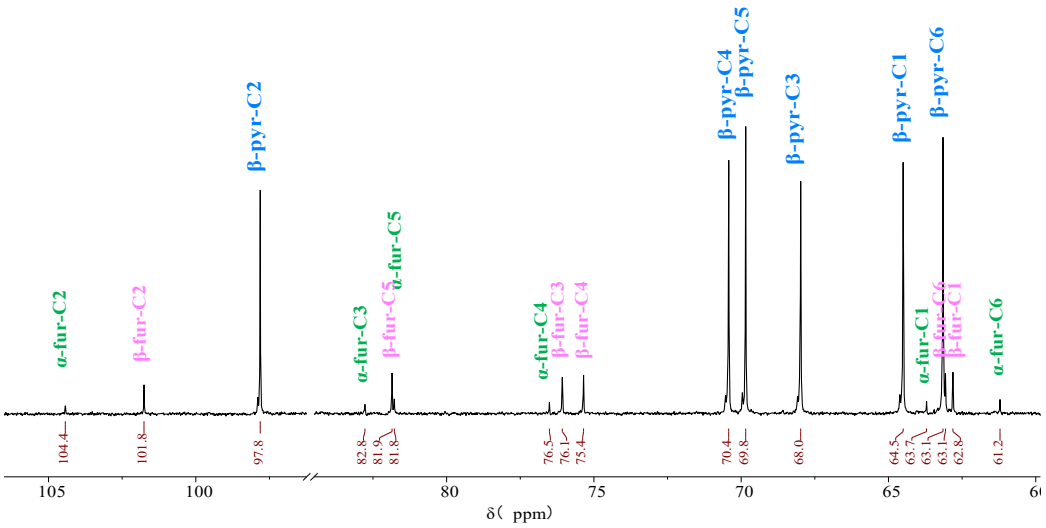

Figure S2. ^{13}C NMR spectrum for fructose in methanol-d_4. Conditions: 50 mg fructose in 0.5 mL methanol-d_4, the supernatant of the dissolved fraction was taken, ns = 1024. * The signals we labelled are three main tautomeric forms of fructose in methanol-d_4 and which are possible tautomeric forms in our reaction system.

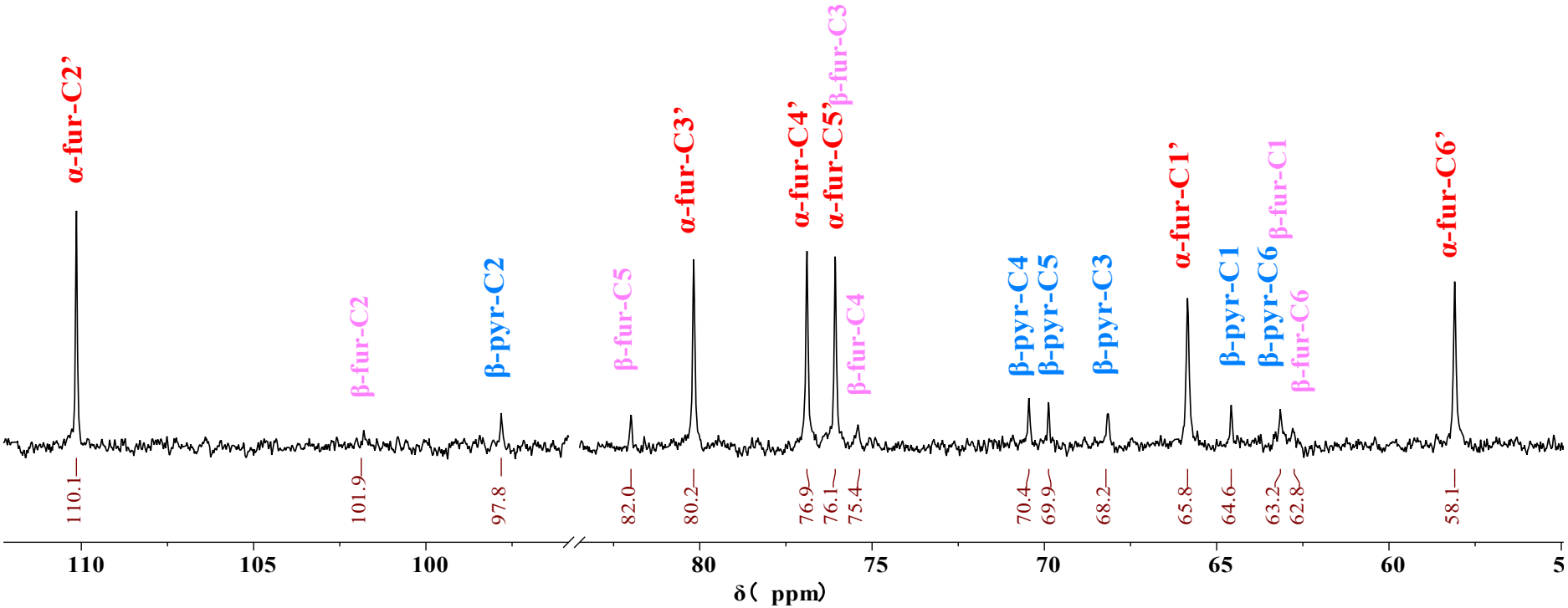

Figure S3. ^{13}C NMR spectrum for fructose with $CaCl_2$ and Et_3N in methanol-d_4. Conditions: 50 mg fructose with equimolar $CaCl_2$ and Et_3N in 0.5 mL methanol-d_4, ns = 1024.

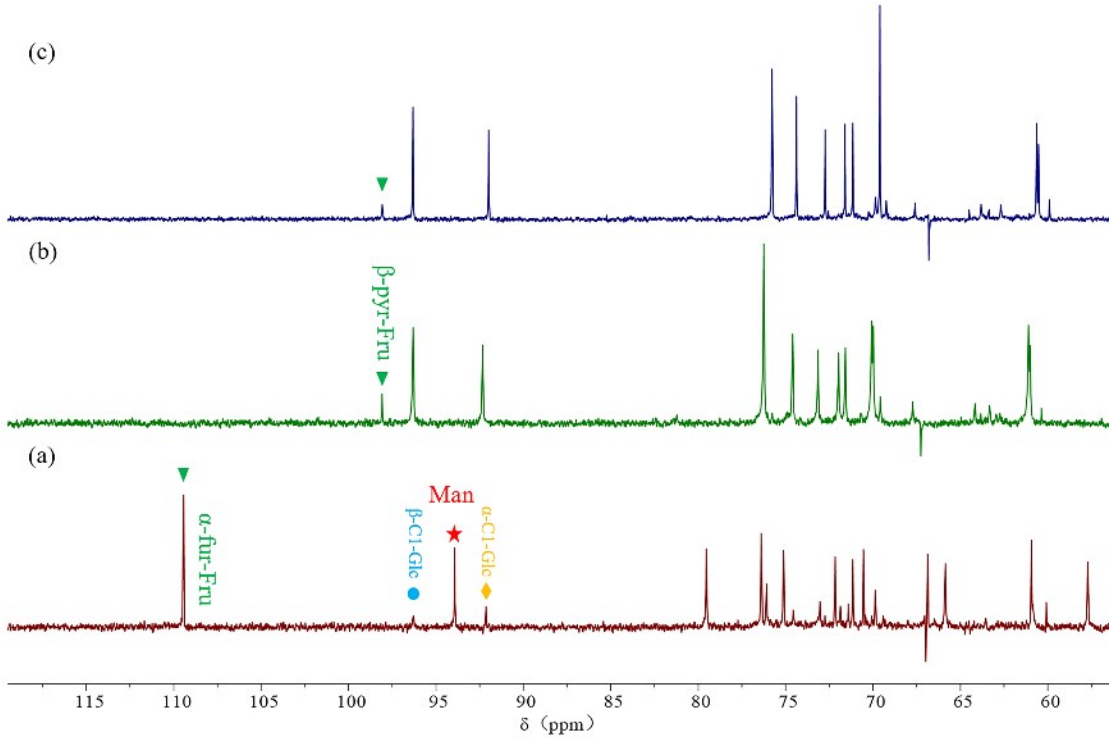

Figure S4. ^{13}C NMR spectra of the reaction mixture where glucose conversion is promoted by (a) $CaCl_2$ and Et_3N, (b) $MgCl_2$ and Et_3N (c) $BaCl_2$ and Et_3N. Reaction conditions: 100 mg glucose with equimolar metal salts and Et_3N as reagents in 1 mL methanol at 65 °C for 1.5 h.

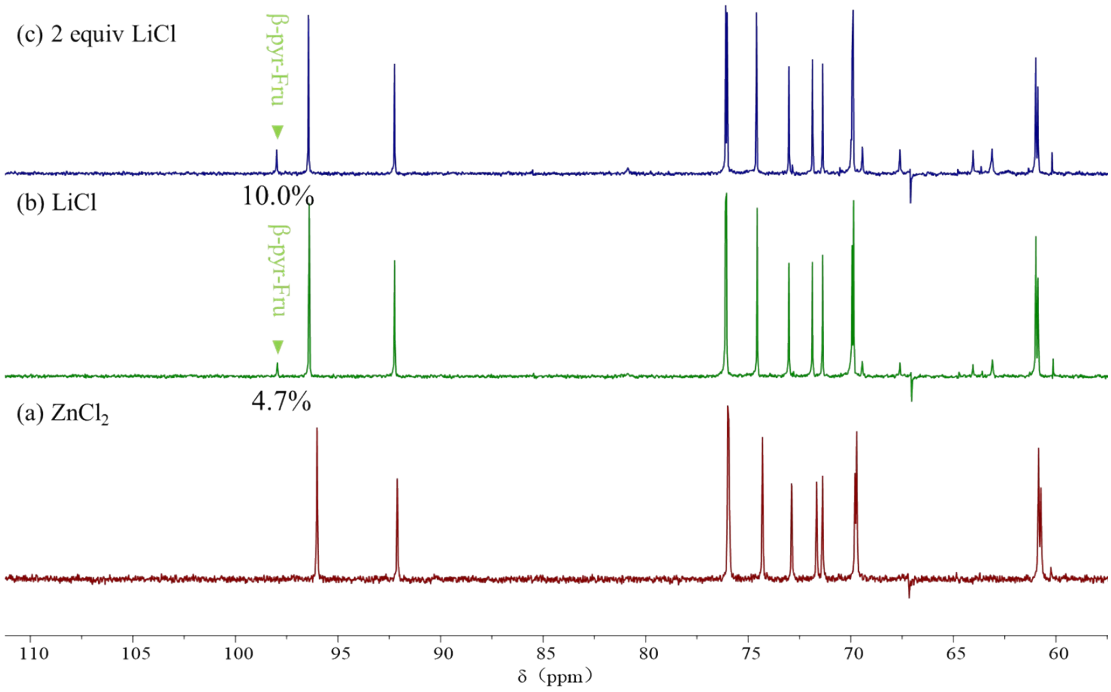

Figure S5. ^{13}C NMR spectra of the reaction mixture where glucose conversion is promoted by (a) equimolar $ZnCl_2$ and Et_3N, (b) equimolar LiCl and Et_3N, (c) 2 equivalent LiCl and equimolar Et_3N. Reaction conditions: 100 mg glucose with metal salts and Et_3N in 1 mL methanol at 65 °C for 1.5 h.

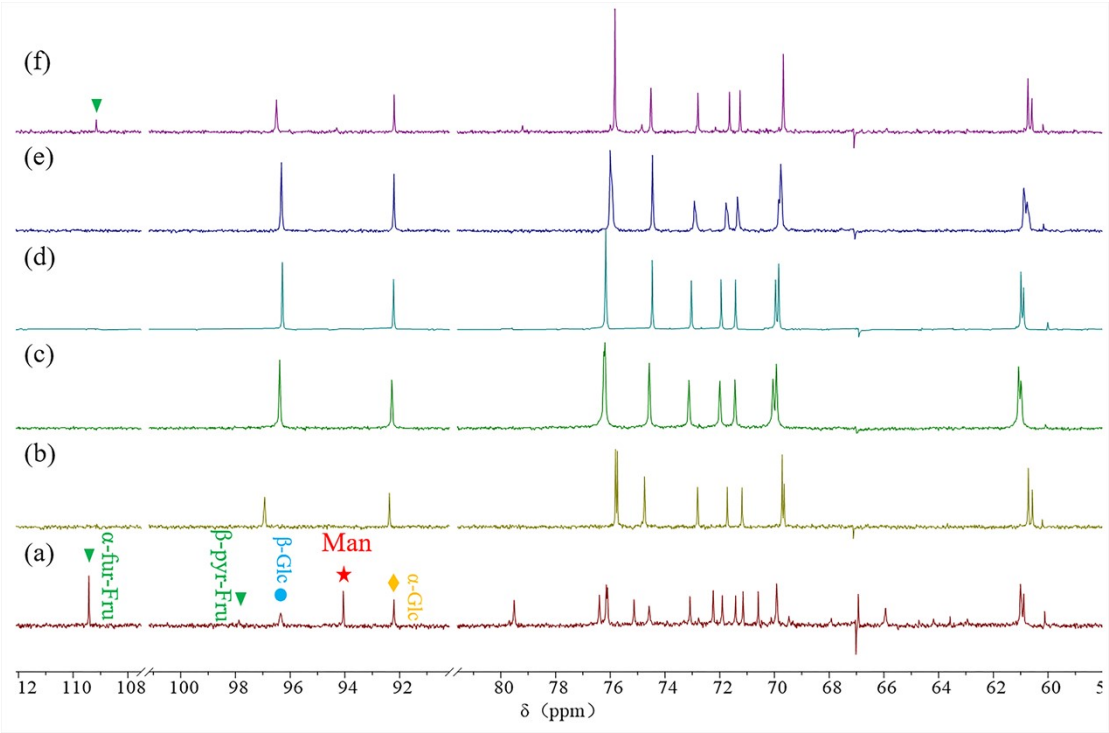

Figure S6. ^{13}C NMR spectra of the reaction mixture where glucose conversion is promoted by (a) $Ca(NO_3)_2$, (b) $Ca(OAc)_2$, (c) $CaSO_4$, (d) $Ca(HPO_4)_2$, (e) $Ca_3(PO_4)_2$, (f) $Ca(OAc)_2$+2NaCl and Et_3N. Reaction conditions: 100 mg glucose with equimolar calcium salts and Et_3N as reagents in 1 mL methanol at 65 °C for 1.5 h.

Table S1. The effect of different metal salts in glucose isomerization

Mental salt	Y_{fru}[a] (%)	Y_{man}[b] (%)
$CaCl_2$	39	29
$MgCl_2$	7	-[c]
$BaCl_2$	9	-
$Ca(NO_3)_2$	23	18
$Ca(OAc)_2$	-	-
$Ca(OAc)_2$+2NaCl	5	5
$CaSO_4$	-	-
$Ca(HPO_4)_2$	-	-
$Ca_3(PO_4)_2$	-	-

Reaction conditions: 100 mg glucose with equimolar mental salts and Et_3N in methanol at 65 °C for 1.5 h.
[a] The yield of fructose.
[b] The yield of mannose.
[c] Not detected under the present condition by NMR spectroscopy.

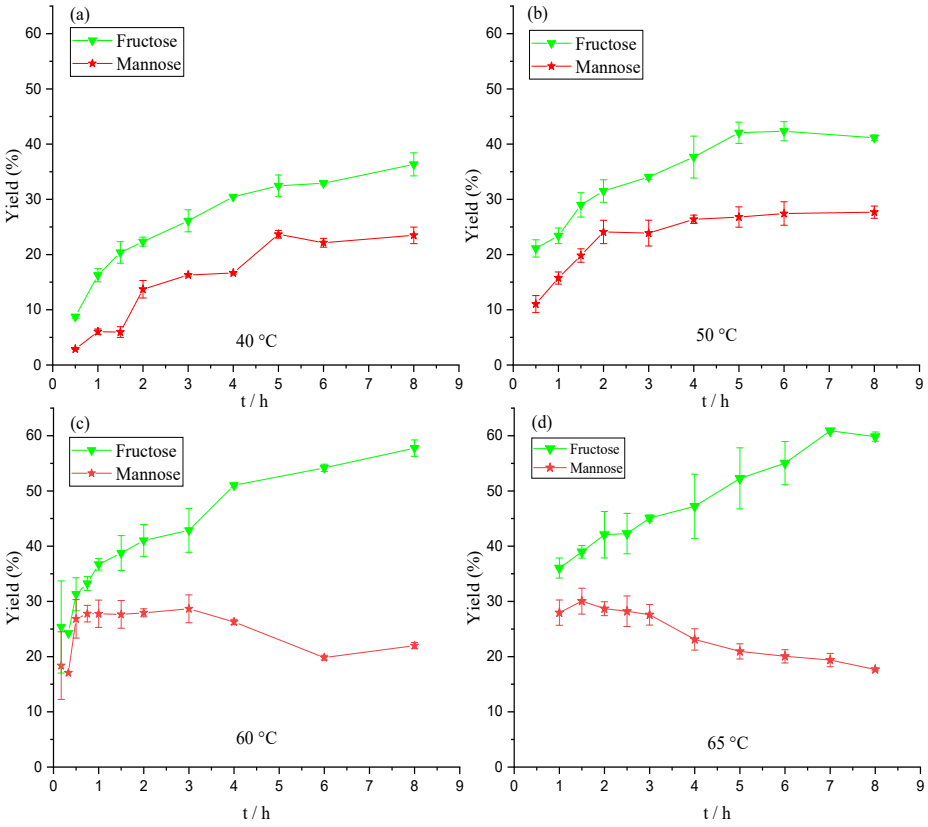

F

igure S7. Isomerization of glucose in methanol at (a) 40 °C, (b) 50 °C, (c) 60 °C, (d) 65 °C. Reaction conditions: 100 mg/mL glucose in methanol with equimolar of $CaCl_2$ and Et_3N.

Table S2. Isomerization of Glucose to fructose by various of chemical catalysts and reagents

Catalyst	Solvent	T (°C)	t (min)	Yield	Selectivity	Ref
$CrCl_3$	H_2O	120	180	25.4	48.6	[1]
$AlCl_3$	H_2O	120	180	26.3	82.7	[1]
$SnCl_4$	H_2O	120	180	4.7	26	[1]
$ZnCl_2$	H_2O	120	15	0	0	[2]
LiCl	H_2O	120	15	7.7	81	[2]
LiBr	H_2O	120	15	30.3	58.5	[2]
$CaBr_2$	H_2O	120	15	22.4	23.7	[2]
Ti-Beta	H_2O	100	120	11	61	[3]
Ti-Beta	MeOH	100	120	8	22	[4]
KOH	H_2O	78	60	11	61	[5]
morpholine	H_2O	100	30	17	43	[6]
piperazine	H_2O	100	30	28	62	[6]
ethylenediamine	H_2O	100	30	25	60	[6]
triethylamine	H_2O	100	30	31	54	[6]
piperidine	H_2O	100	30	29	51	[6]
pyrrolidine	H_2O	100	30	29	59	[6]
arginine	H_2O	120	15	31	76	[6]
CaO/ZrO_2	H_2O	160	15	21	70	[7]
$NaAlO_2$	H_2O	55	180	41	70	[8]
ZrC	H_2O	120	20	34	76	[9]
Al-hydrochar	acetone/H_2O	160	20	25	60	[10]
CeO_2/ATP	H_2O	100	200	36.4	79.1	[11]
Mg-C_3N_4	H_2O	80	240	32	84	[12]
aniline	H_2O	90	120	10.6	67.7	[13]
acetoxime	H_2O	90	120	7.6	24.8	[13]
diacetyldioxime	H_2O	90	120	10.3	54.6	[13]
diacetylmonoxime	H_2O	90	120	24.3	52.0	[13]
Sn-Beta	H_2O	120	60	46	70	[3]
Sn-Al-Beta	H_2O	120	60	43	65	[3]
H-USY	MeOH/H_2O	120	60	55	76	[14]
Mg–Al Hydrotalcite	MeOH	100	300	51	72	[15]
Al-MOF	EtOH	120	240	52	64	[16]
amidoximated polyacrylonitrile	H_2O	85	300	48.9	98.6	[13]
Modified Zirconium UiO-66	i-PrOH/H_2O*	90	-	56	72	[17]
Sn-SPP(186)	EtOH/H_2O*	90	1800	65	74	[18]

* Hydrolysis is required after the reaction.

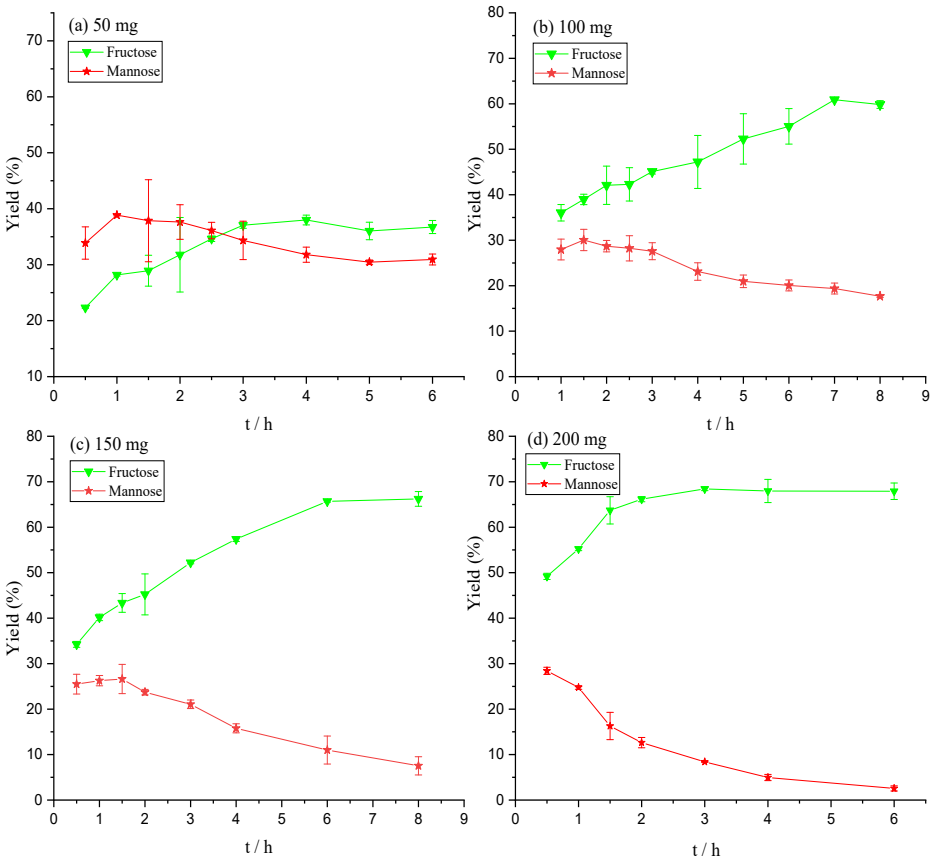

Figure S8. The effect of initial glucose concentration on isomerization. (a) 50 mg/mL, (b) 100 mg/mL, (c) 150 mg/mL, (d) 200 mg/mL. Reaction conditions: different concentration of glucose in methanol with equimolar $CaCl_2$ and Et_3N at 65 °C.

Table S3. The effect of the ratio between $CaCl_2$ and glucose on isomerization

t / h	0.5 $CaCl_2$		1.0 $CaCl_2$		1.5 $CaCl_2$		2.0 $CaCl_2$	
	Y_{fru} (%)	Y_{man} (%)	Y_{fru} (%)	Y_{man} (%)	Y_{fru} (%)	Y_{man} (%)	Y_{fru} (%)	Y_{man} (%)
0.5	18	20	29	27	43	28	52	24
1.0	20	21	36	28	46	29	60	16
1.5	23	22	39	30	50	24	62	16
2.0	24	23	42	29	56	21	62	12
3.0	26	24	45	28	58	15	62	13

Reaction conditions: 100 mg/mL glucose with different ratio of $CaCl_2$ and equimolar Et_3N as reagents in methanol at 65 °C. *Considering its solubility, the initial concentration of glucose was set as 100 mg/mL.

Table S4. The effect of the ratio between Et_3N and glucose on isomerization

t / h	0.5 Et_3N		1.0 Et_3N		1.5 Et_3N		2.0 Et_3N	
	Y_{fru} (%)	Y_{man} (%)	Y_{fru} (%)	Y_{man} (%)	Y_{fru} (%)	Y_{man} (%)	Y_{fru} (%)	Y_{man} (%)
0.5	16	13	29	27	40	32	45	26
1.0	18	14	36	28	42	26	54	22
1.5	21	15	39	30	53	18	59	13
2.0	23	18	42	29	60	14	65	9
3.0	25	18	45	28	61	11	61	4

Reaction conditions: 100 mg/mL glucose with different ratio of Et_3N and equimolar $CaCl_2$ as reagents in methanol at 65 °C.

Table S5. The effect of solvent in glucose isomerization with $CaCl_2$ and Et_3N as reagents

Solvent	Temperature/°C	C_{glc}[a] (%)	Y_{fru}[b] (%)
water	65	25	18
ethanol	65	81	42
ethylene glycol	65	*[c]	-[d]
γ-butyrolactone	65	*	-
γ-butyrolactone	85	8	5
γ-butyrolactone	135	43	19

Reaction conditions: 100 mg glucose with equimolar $CaCl_2$ and Et_3N as reagents.

[a] The conversion of glucose.

[b] The yield of fructose.

[c] Unable to determine the exact value of conversion.

[d] Not detected under the present condition by NMR technology.

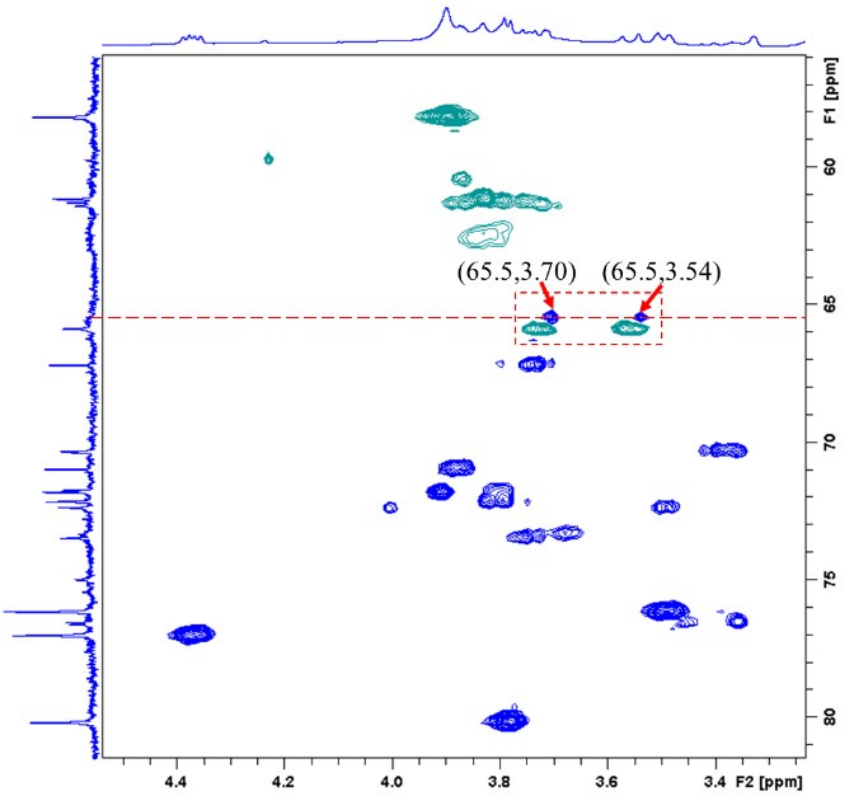

Figure S9. ^{1}H-^{13}C HSQC NMR spectrum of sugar fractions obtained from the isomerization of glucose promoted by Et_3N and $CaCl_2$ in methanol-d_4.

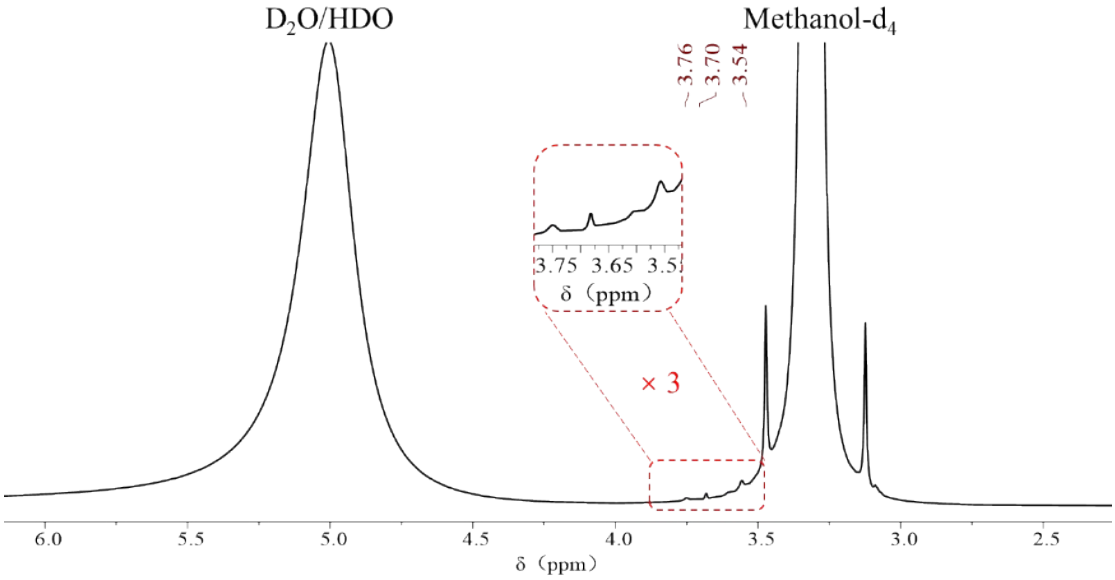

Figure S10. ^{2}H NMR spectrum of reaction mixture obtained from the isomerization of glucose promoted by Et_3N and $CaCl_2$ in methanol-d_4.

Path I

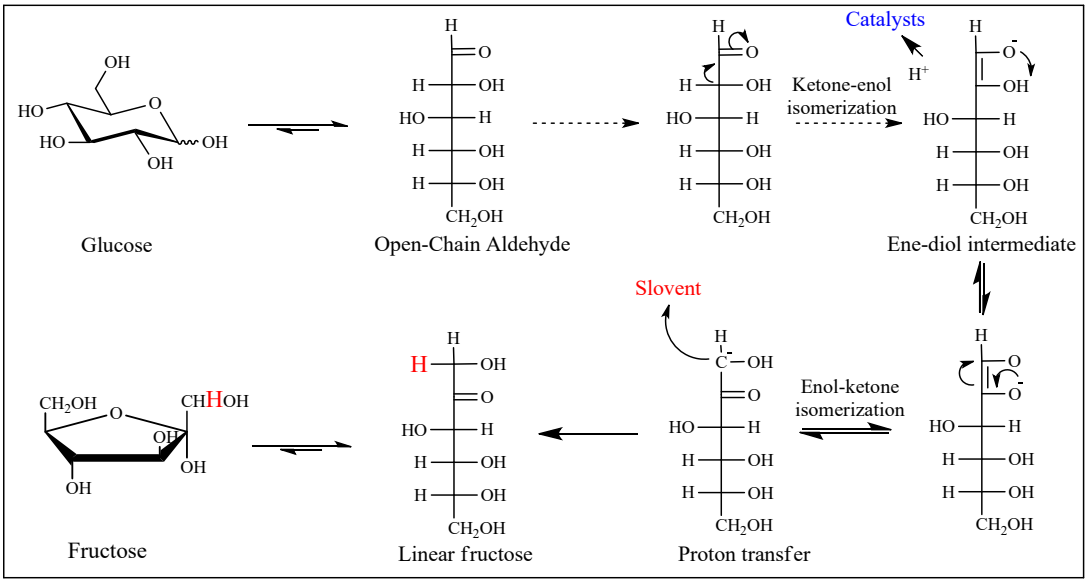

Path II

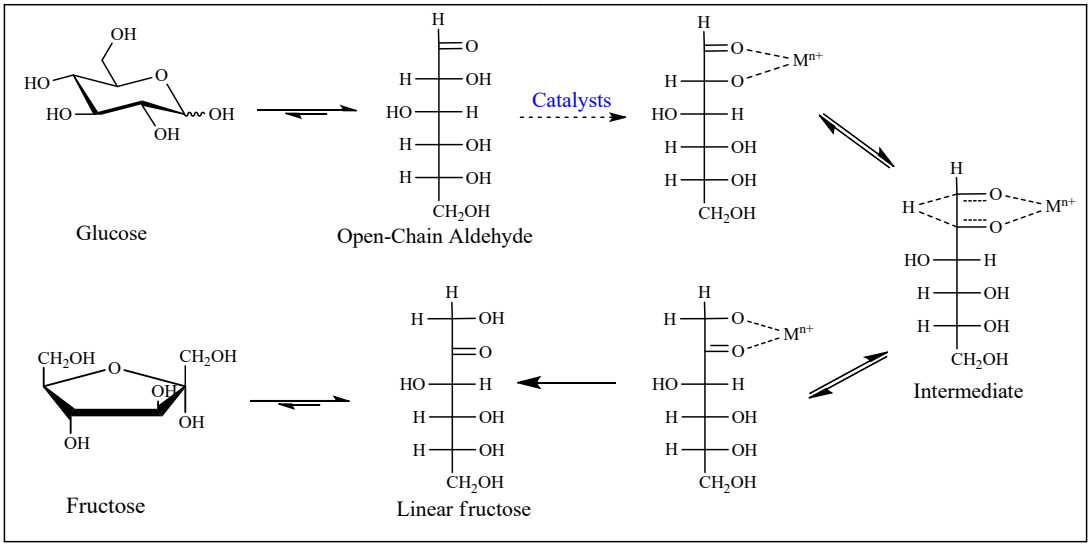

Scheme S1. Proposed glucose isomerization reaction pathways.

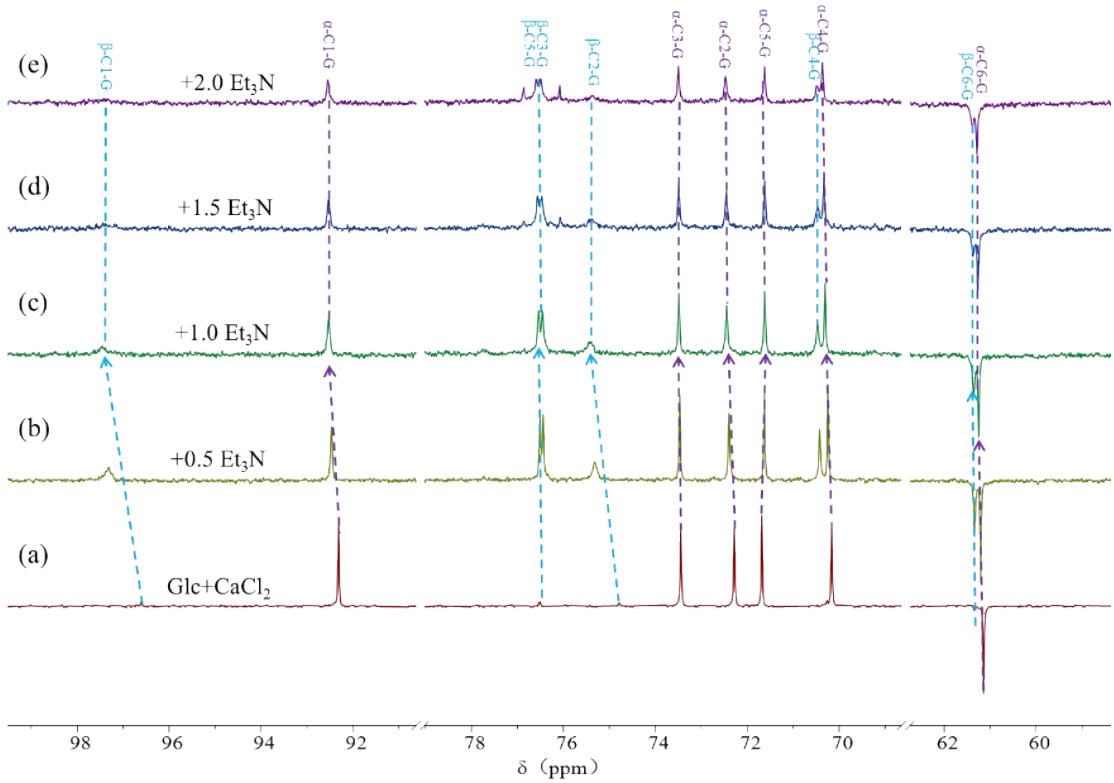

Figure S11. The DEPT135 stacked NMR spectra with different molar ratios of Et_3N to glucose- $CaCl_2$ in methanol-d_4.

Conditions: 50 mg/mL glucose and equimolar $CaCl_2$ with different molar ratios of Et_3N in methanol-d_4, 25 °C.

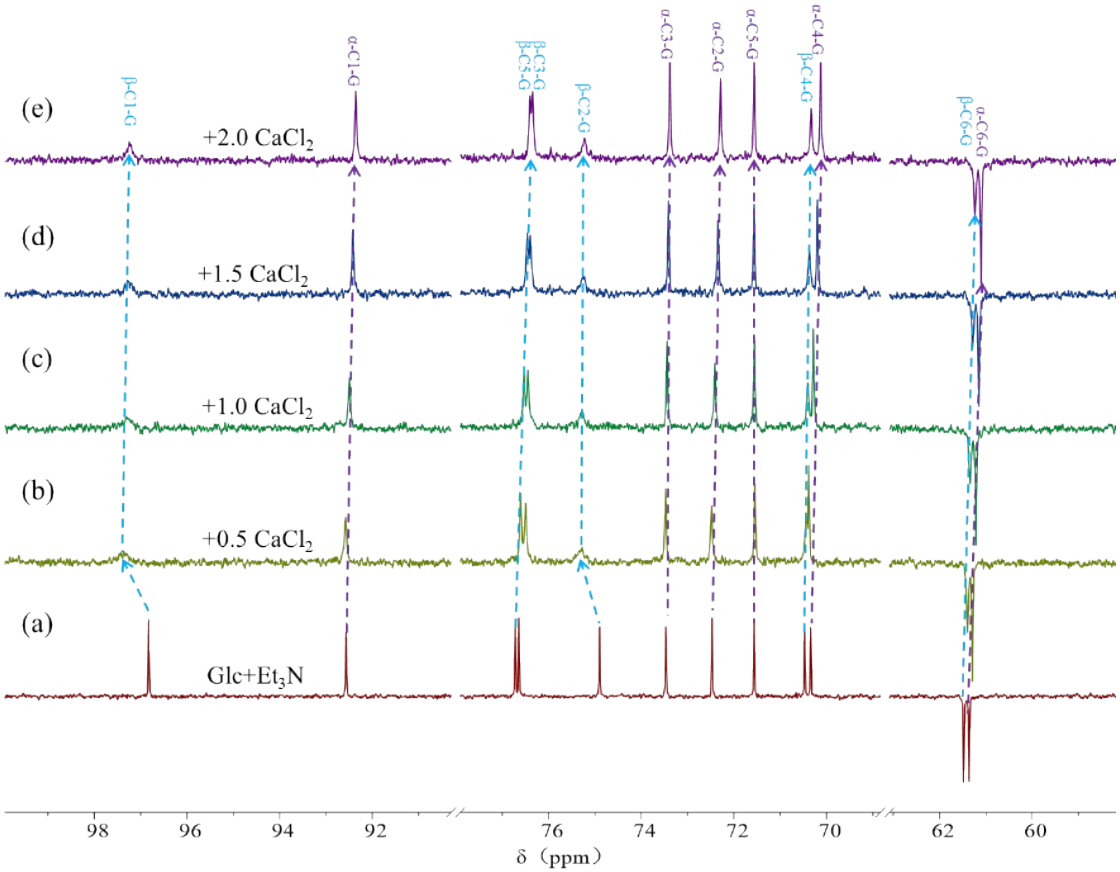

Figure S12. The DEPT135 stacked NMR spectra with different molar ratios of $CaCl_2$ to glucose-Et_3N in methanol-d_4.

Conditions: 50 mg/mL glucose and equimolar Et_3N with different molar ratios of $CaCl_2$ in methanol-d_4, 25 °C.

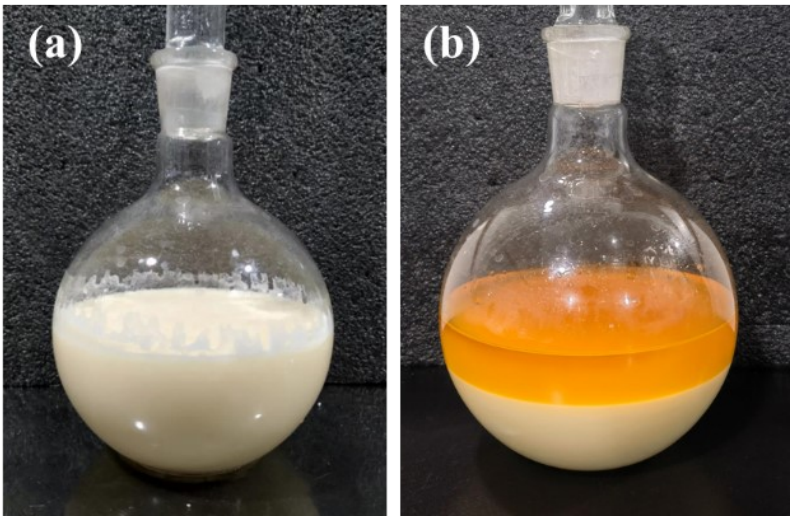

Figure S13. Photograph of the reaction mixtures. (a) The mixture that just finished reacting; (b) The mixture that cooled for a while.

Reaction conditions: 5 g glucose with equimolar Et_3N and two equivalent $CaCl_2$ as reagents at 65 °C in methanol for 1 h.

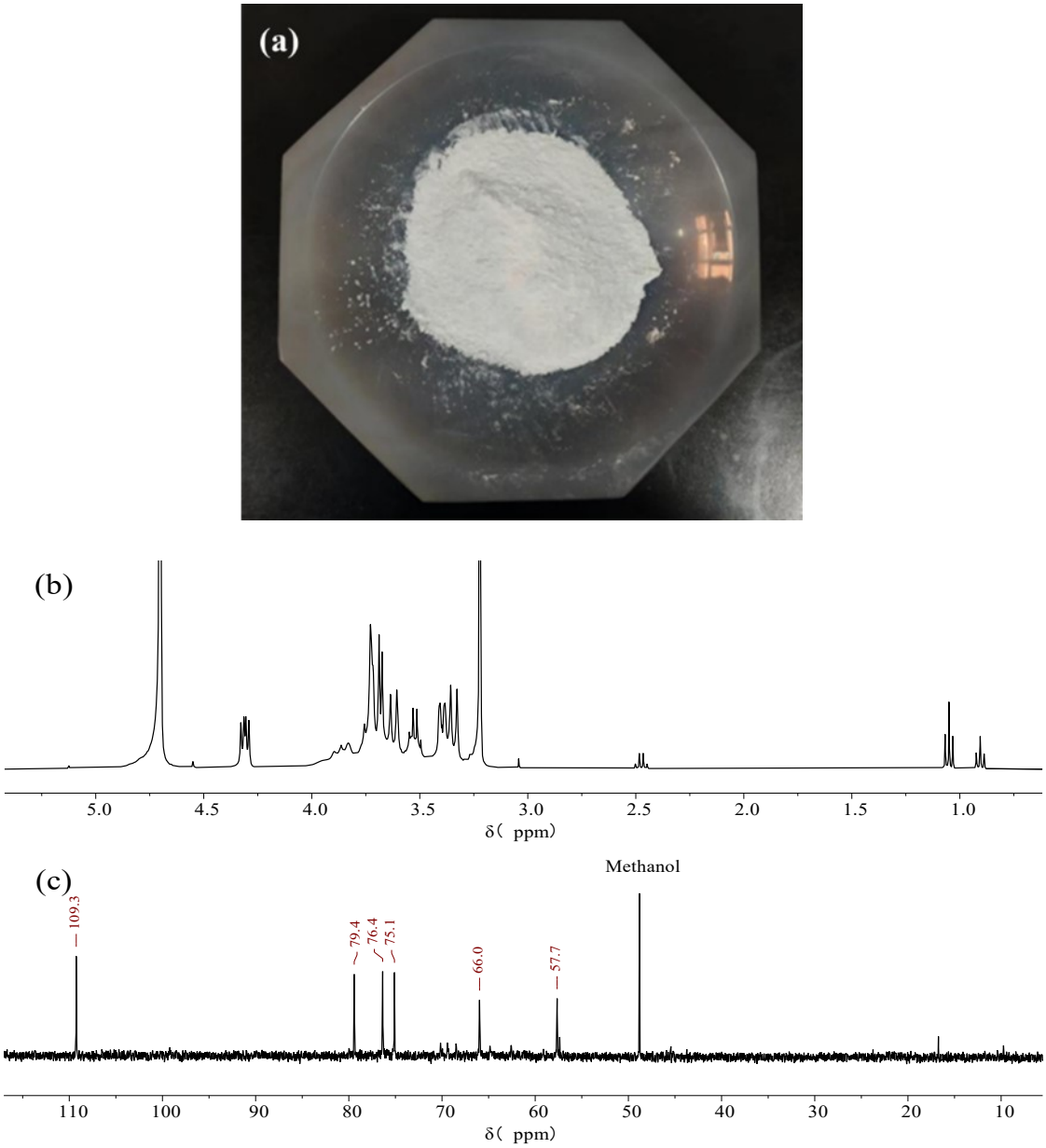

Figure S14. (a) Photograph, (b) ^{1}H NMR spectrum, (c) ^{13}C NMR spectrum of the dried sample.

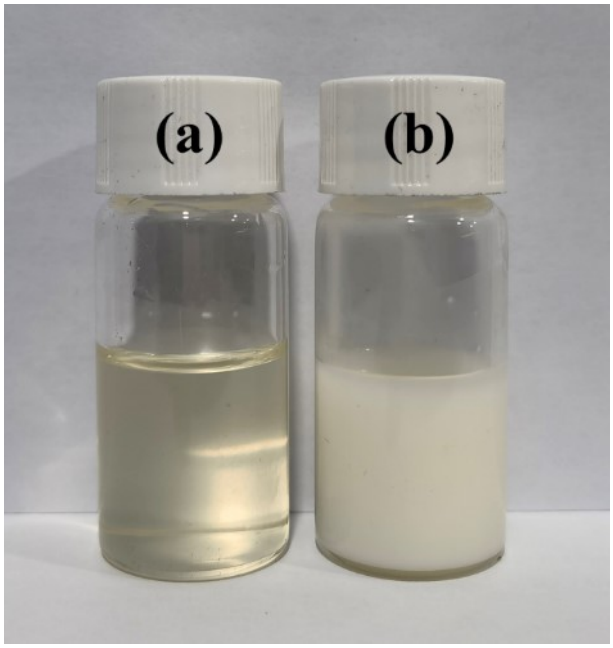

Figure S15. Photograph of the dried product dissolved in water. (a) the solution before bubbling CO_2; (b) the solution after bubbling CO_2.

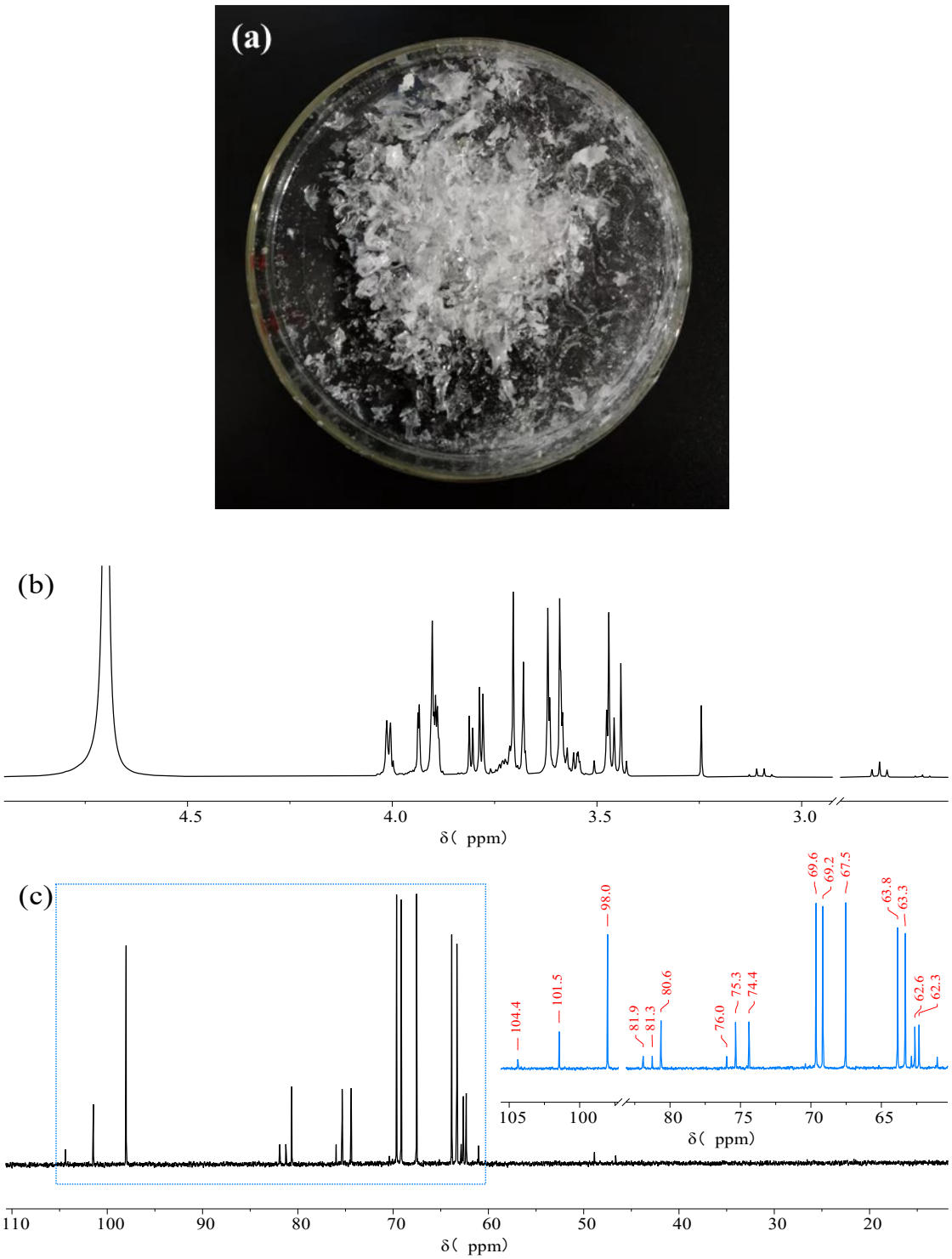

Figure S16. (a) Photograph, (b) ^{1}H NMR spectrum, (c) ^{13}C NMR spectrum of the purified fructose with 45% isolated yield.

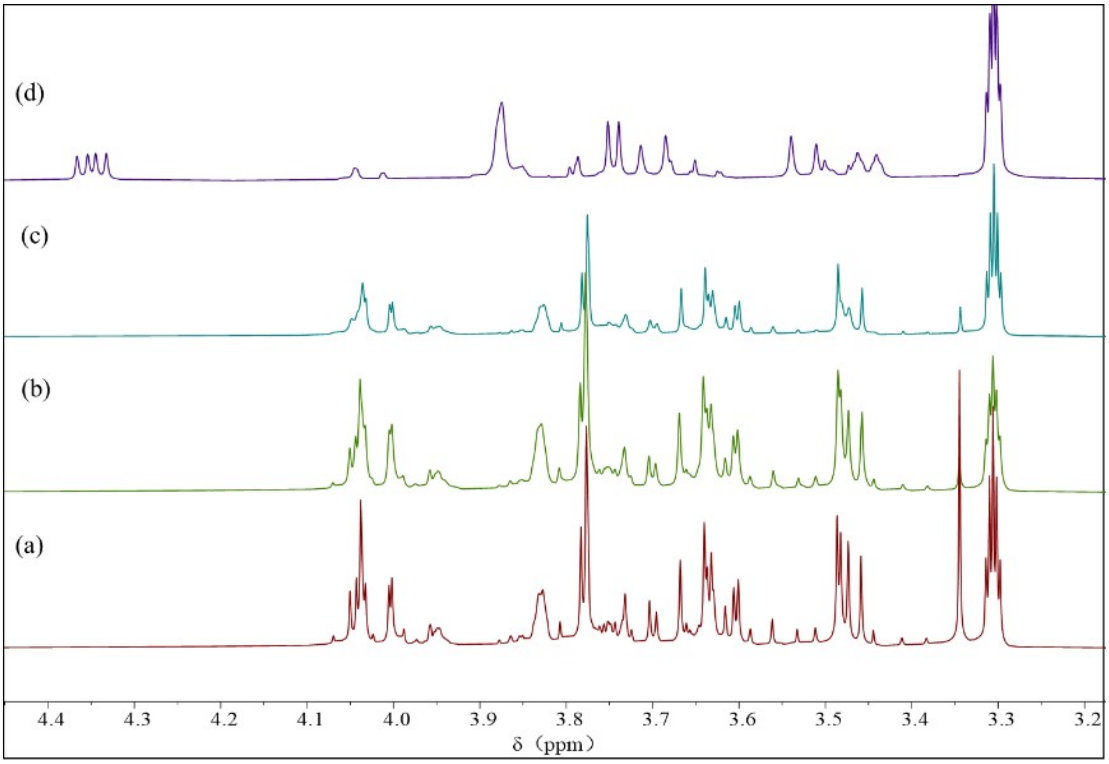

Figure S17. (a) ^{1}H NMR spectrum of sugar fractions obtained from the (a) fructose, (b) fructose with equimolar $CaCl_2$, (c) fructose with equimolar Et_3N, (d) fructose with equimolar $CaCl_2$ and Et_3N. Conditions: 5 mg fructose in 0.5 mL methanol-d_4 at 25 °C.

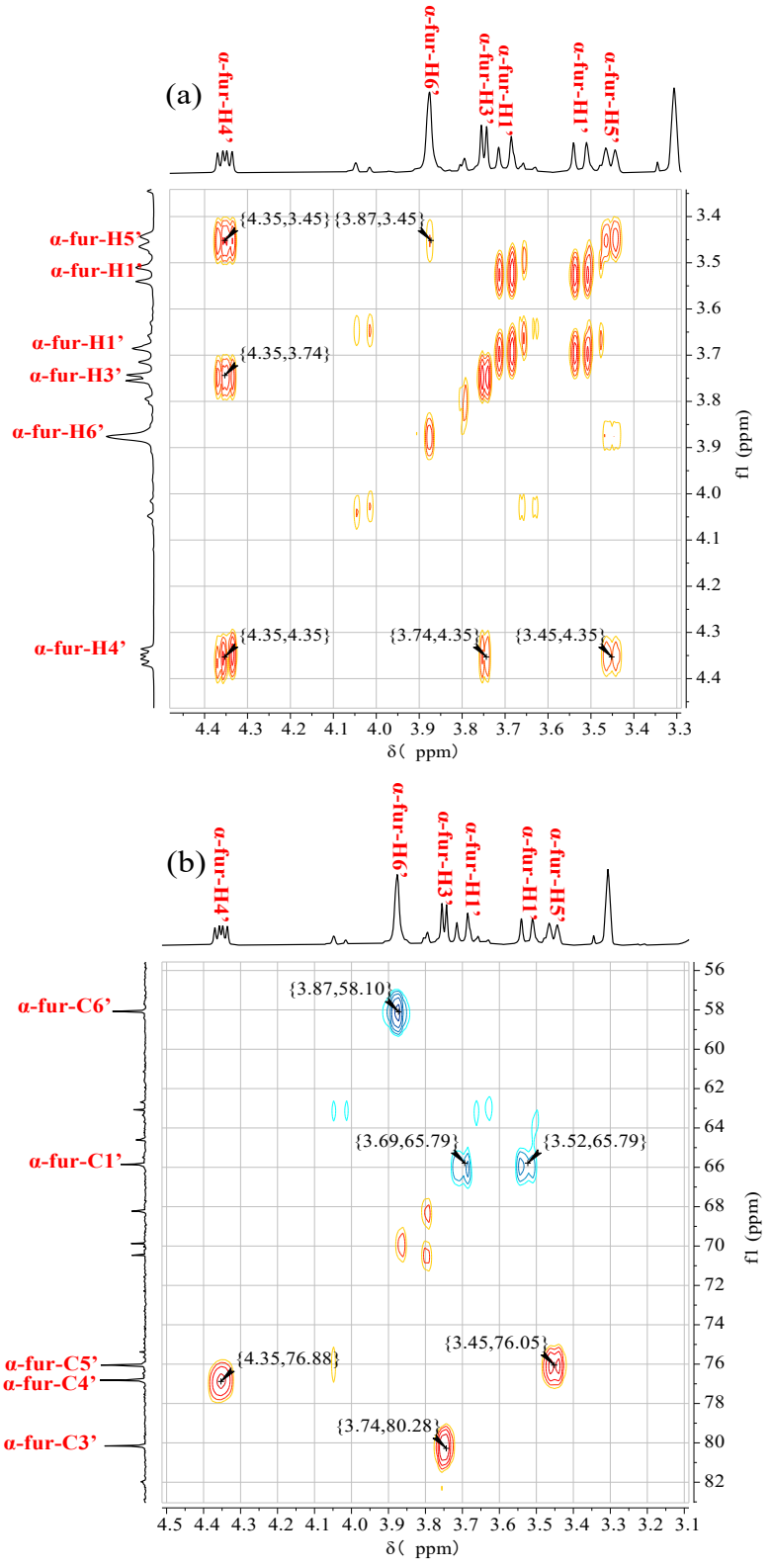

Figure S18. (a) ^{1}H-^{1}H COSY NMR, (b) ^{1}H-^{13}C HSQC NMR spectra of sugar fractions obtained from fructose mixed with Et_3N and $CaCl_2$ in methanol-d_4.

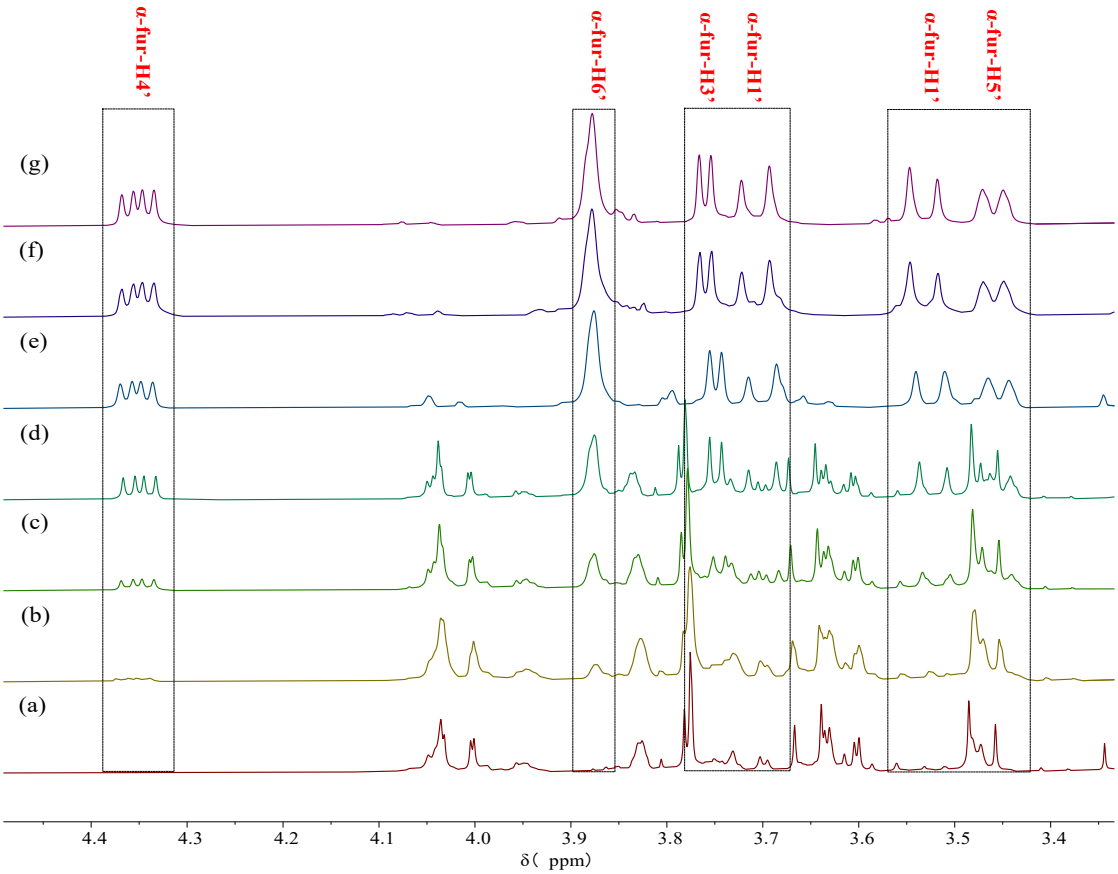

Figure S19. The ^{1}H stacked NMR spectra with different molar ratios of $CaCl_2$ to fructose in methanol-d_4. (a) fructose: $CaCl_2$: Et_3N = 1:0:1, (b) fructose: $CaCl_2$: Et_3N = 1:0.1:1, (c) fructose: $CaCl_2$: Et_3N = 1:0.25:1, (d) fructose: $CaCl_2$: Et_3N = 1:0.5:1, (e) fructose: $CaCl_2$: Et_3N = 1: 1:1, (f) fructose: $CaCl_2$: Et_3N = 1:1.5:1, (g) fructose: $CaCl_2$: Et_3N = 1:2:1. Conditions: 12.5 mg/mL fructose in methanol-d_4, 25 °C.

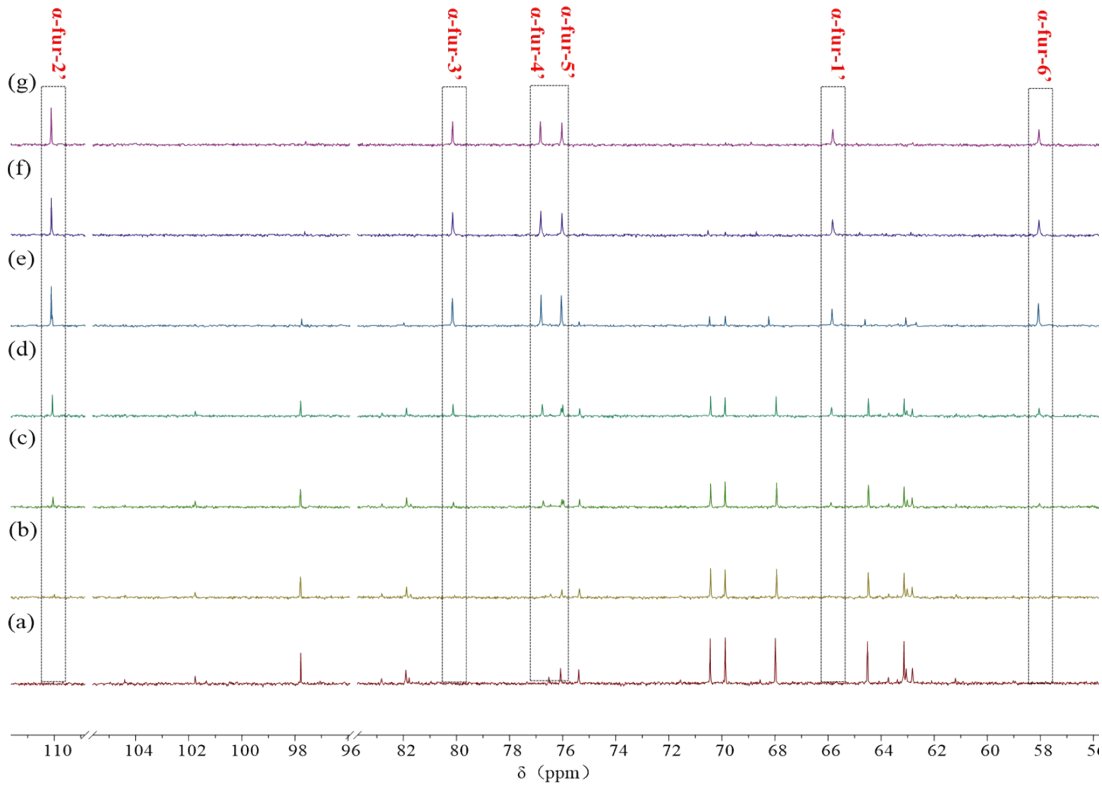

Figure S20. The ^{13}C stacked NMR spectra with different molar ratios of $CaCl_2$ to fructose in methanol-d_4. (a) fructose: Et_3N: $CaCl_2$=1:1:0, (b) fructose: Et_3N: $CaCl_2$=1:1:0.1, (c) fructose: Et_3N: $CaCl_2$=1:1:0.25, (d) fructose: Et_3N: $CaCl_2$=1:1:0.5, (e) fructose: Et_3N: $CaCl_2$=1:1:1, (f) fructose: Et_3N: $CaCl_2$=1:1:1.5, (g) fructose: Et_3N: $CaCl_2$=1:1:2. Conditions: 12.5 mg/mL fructose in methanol-d_4, 25 °C.

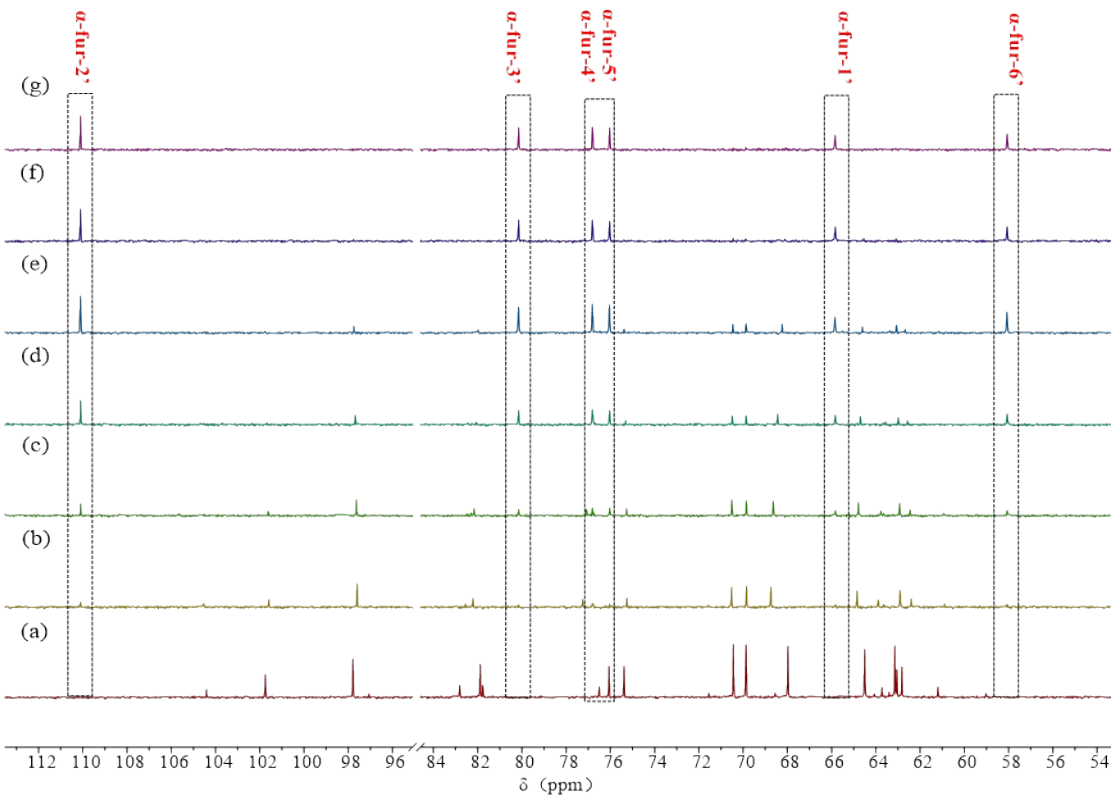

Figure S21. The ^{13}C stacked NMR spectra with different molar ratios of Et_3N to fructose in methanol-d_4. (a) fructose: $CaCl_2$: Et_3N = 1:1:0, (b) fructose: $CaCl_2$: Et_3N = 1:1:0.1, (c) fructose: $CaCl_2$: Et_3N = 1:1:0.25, (d) fructose: $CaCl_2$: Et_3N = 1:1:0.5, (e) fructose: $CaCl_2$: Et_3N = 1:1:1, (f) fructose: $CaCl_2$: Et_3N = 1:1:1.5, (g) fructose: $CaCl_2$: Et_3N = 1:1:2. Conditions: 12.5 mg/mL fructose in methanol-d_4, 25 °C.

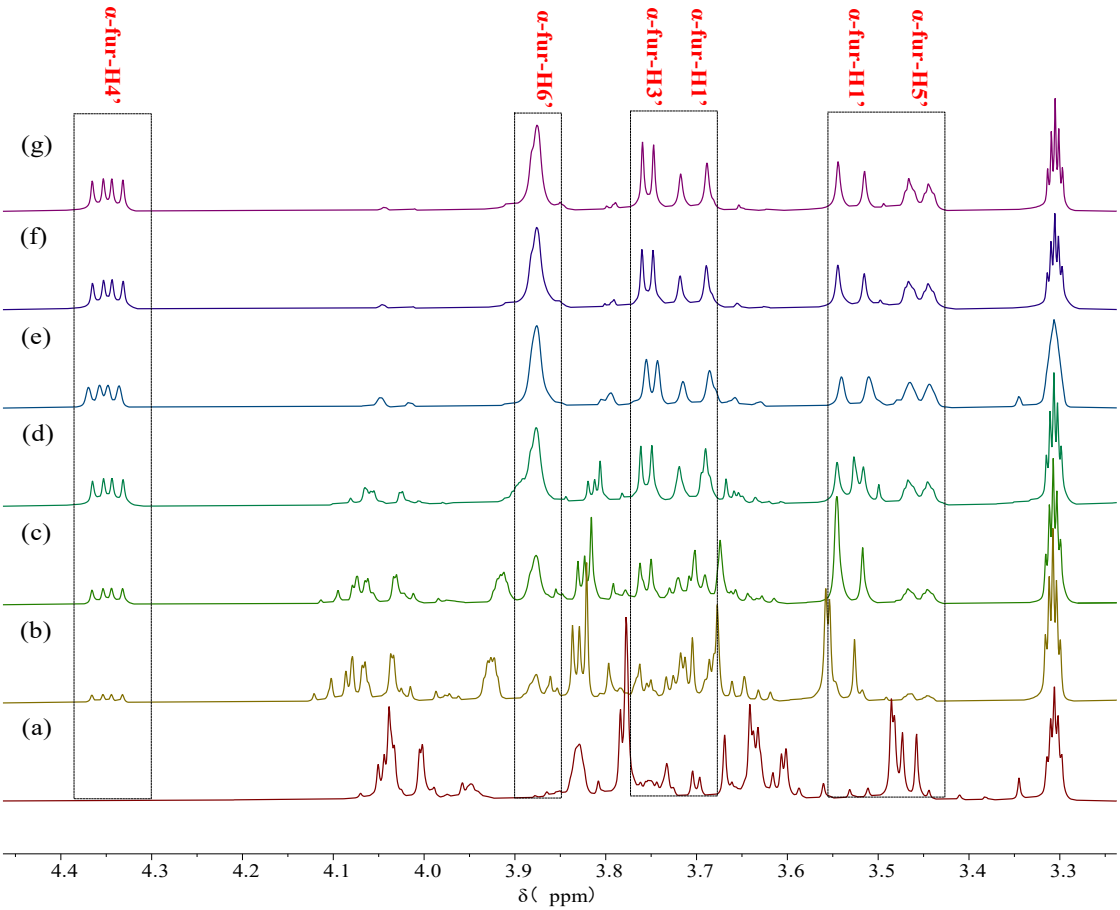

Figure S22. The ^{1}H stacked NMR spectra with different molar ratios of Et_3N to fructose in methanol-d_4. (a) fructose: $CaCl_2$: Et_3N = 1:1:0, (b) fructose: $CaCl_2$: Et_3N = 1:1:0.1, (c) fructose: $CaCl_2$: Et_3N = 1:1:0.25, (d) fructose: $CaCl_2$: Et_3N = 1:1:0.5, (e) fructose: $CaCl_2$: Et_3N = 1:1:1, (f) fructose: $CaCl_2$: Et_3N = 1:1:1.5, (g) fructose: $CaCl_2$: Et_3N = 1:1:2. Conditions: 12.5 mg/mL fructose in methanol-d_4, 25 °C.

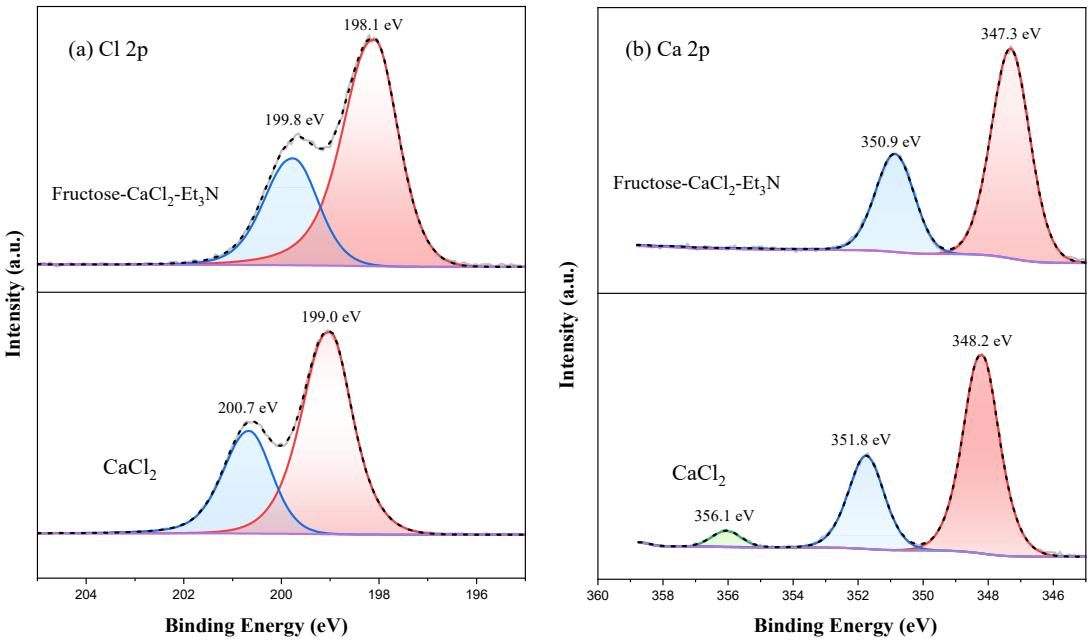

Figure S23. (a) Cl 2p and (b) Ca 2p XPS patterns of fructose-$CaCl_2$-Et_3N samples.

References:

S1. J. Q. Tang, X. W. Guo, L. F. Zhu and C. W. Hu, *ACS Catal.*, 2015, **5**, 5097-5103.

S2. C. G. Yoo, N. Li, M. Swannell and X. Pan, *Green Chem.*, 2017, **19**, 4402-4411.

S3. M. Liu, S. Jia, C. Li, A. Zhang, C. Song and X. Guo, *Chin. J. Catal.*, 2014, **35**, 723-732.

S4. R. Gounder and M. E. Davis, *ACS Catal.*, 2013, **3**, 1469-1476.

S5. A. P. C. K. J. M. de Bruijn, H. van Bekkum, *Recl. Trav. Chim. Pays-Bas*, 1987, **106**, 35-43.

S6. C. Liu, J. M. Carraher, J. L. Swedberg, C. R. Herndon, C. N. Fleitman and J.-P. Tessonnier, *ACS Catal.*, 2014, **4**, 4295-4298.

S7. H. Kitajima, Y. Higashino, S. Matsuda, H. Zhong, M. Watanabe, T. M. Aida and R. L. Smith, *Catal. Today*, 2016, **274**, 67-72.

S8. S. Despax, B. Estrine, N. Hoffmann, J. Le Bras, S. Marinkovic and J. Muzart, *Catal. Commun.*, 2013, **39**, 35-38.

S9. P. A. Son, S. Nishimura and K. Ebitani, *React. Kinet., Mech. Catal.*, 2013, **111**, 183-197.

S10. J. Liu, X. Zhang, L. Yang, U. A. Danhassan, S. Zhang, M. Yang, K. Sheng and X. Zhang, *Sci. Total Environ.*, 2021, **777**, 146037.

S11. B. Li, H. Jiang, X. Zhao, Z. Pei and Q. Zhang, *ChemistrySelect*, 2020, **5**, 14971-14977.

S12. M. Laiq Ur Rehman, Q. Hou, X. Bai, Y. Nie, H. Qian, T. Xia, R. Lai, G. Yu and M. Ju, *ACS Sustainable Chem. Eng.*, 2022, **10**, 1986-1993.

S13. H. Huang, X. G. Meng, W. W. Yu, L. Y. Chen and Y. Y. Wu, *ACS Omega*, 2021, **6**, 19860-19866.

S14. S. Saravanamurugan, M. Paniagua, J. A. Melero and A. Riisager, *J. Am. Chem. Soc.*, 2013, **135**, 5246-5249.

S15. S. An, D. Kwon, J. Cho and J. C. Jung, *Catalysts*, 2020, **10**, 1236.

S16. M. S. Rahaman, S. Tulaphol, A. Hossain, J. B. Jasinski, S. B. Lalvani, M. Crocker, T. Maihom and N. Sathitsuksanoh, *ChemCatChem*, 2022, **14**, e202200129.

S17. M. D. d. Mello and M. Tsapatsis, *ChemCatChem*, 2018, **10**, 2417–2423.

S18. L. Ren, Q. Guo, P. Kumar, M. Orazov, D. Xu, S. M. Alhassan, K. A. Mkhoyan, M. E. Davis and M. Tsapatsis, *Angew Chem Int Ed Engl*, 2015, **54**, 10848-10851.